Journal of Colloid and Interface Science 625 (2022) 743–749

Contents lists available at ScienceDirect

Journal of Colloid and Interface Science

journal homepage: www.elsevier.com/locate/jcis

Photochemical approach for multiplexed biofunctionalisation of gallium arsenide

Bárbara Santos Gomes *, Francesco Masia

School of Biosciences, Cardiff University, Cardiff CF10 3AX, United Kingdom

GRAPHICAL ABSTRACT

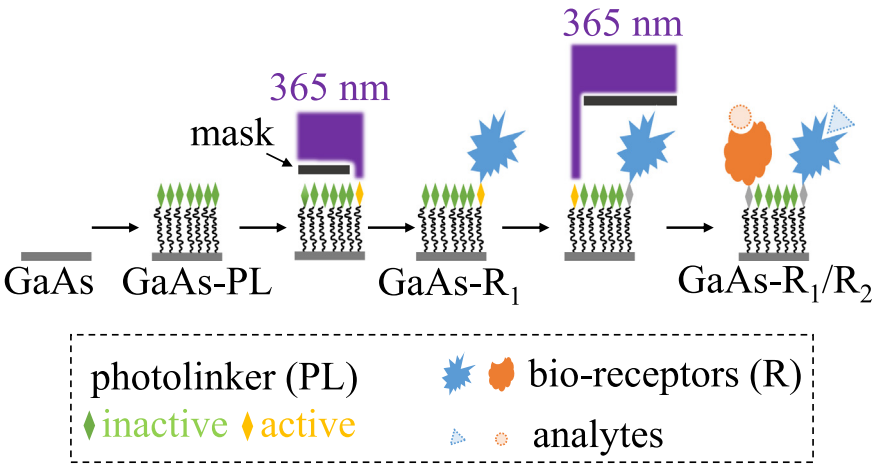

ARTICLE INFO

Article history:
Received 29 March 2022
Revised 1 June 2022
Accepted 17 June 2022
Available online 20 June 2022

Keywords:
Neutravidin
X-ray photoelectron spectroscopy
Self-assembled monolayer
Protein non-specific binding
Optical biosensor
Compound semiconductor
Alkanethiolate film
Carbodiimide chemistry
Diazirine
Photocrosslinker
Ultraviolet light
Carbene

ABSTRACT

The optoelectronic properties of gallium arsenide (GaAs) hold great promise in biosensing applications, currently being held back by the lack of methodologies reporting the spatially selective functionalisation of this material with multiple biomolecules. Here, we exploit the use of a photoreactive crosslinker - a diazirine derivative - for spatially selective covalent immobilisation of multiple bioreceptors on the GaAs surface. As a proof of principle we show the immobilisation of two proteins: neutravidin and endosulfine alpha protein. X-ray photoelectron spectroscopy results showed the presence of the biomolecules on the GaAs regions selectively exposed to ultraviolet light. The approach presented here is applicable to the covalent attachment of other biomolecules, paving the way for using GaAs as a platform for multiplexed biosensing.

* Corresponding author.
E-mail address: SantosGomesB@cardiff.ac.uk (B. Santos Gomes).

https://doi.org/10.1016/j.jcis.2022.06.071
0021-9797/

1. Introduction

The use of photoactive molecules as linkers between a solid support and a biomolecule has been reported for a variety of applications in biotechnology. An example of a successful application of this approach is the creation of complex microarrays of nucleic acids on glass, where nucleotides incorporating photoremovable protective groups are used for in situ synthesis of oligonucleotides (Affymetrix GeneChip® technology). Proteins have also been immobilised on a variety of substrates using light as a facilitator [1–3], for applications such as biosensing, drug delivery and cell behaviour studies. Amongst the most popular photosensitive groups incorporated in crosslinking agents, are the diazirines [4,5], which offer high crosslinking efficiency at long non-destructive wavelength ultraviolet (UV) light. The activation of the diazirine photoreactive group releases nitrogen to produce highly reactive carbene species, with a lifetime in the order of nanoseconds [6], which then bond with nearby functional groups (Fig. S1). Aromatic diazirines are known to produce higher ratios of carbene over the rearranged diazo byproduct (which presents longer lifetime and less reactivity), compared to aliphatic diazirines, and the introduction of a trifluoromethyl group prevents the carbene from undergoing rearrangements [7,8].

Gallium arsenide (GaAs) is a III-V semiconductor which is largely investigated for his optoelectronic properties which make it suitable for several optoelectronic devices such as light sources and photodetectors. GaAs has been recently proposed as platform for biosensing applications [9,10]. Most reports on the functionalisation of the GaAs surface with biomolecules (such as peptides [11], bacteria [12], virus [13] and proteins [14]) are based on the creation of alkanethiolate self-assembled monolayers (SAMs) [11–23], taking advantage of the highly covalent As-S bond [24]. To our knowledge, the use of photoreactive crosslinkers on GaAs surfaces has not yet been reported and neither has the patterned functionalisation of this substrate with multiple biomolecules.

In this study, we focus on a photochemical strategy for the spatially selective immobilisation of multiple proteins on GaAs. We have previously demonstrated the immobilisation of neutravidin on GaAs, by means of thiol-based dual-component SAMs, followed by covalent attachment of a biotin derivative [25]. Herein we develop a simple protocol using a dual-component SAM for the immobilisation of an aromatic diazirine derivative photoreactive crosslinker. We then study the spatially selective immobilisation of two proteins, neutravidin and endosulfine alpha (ENSA) protein, upon exposure to UV light. These results demonstrate the suitability of GaAs as a platform for miniaturised multiplexed biosensing devices.

2. Materials and Methods

2.1. Materials

GaAs wafers were purchased from Wafer Technology with the following specs: prime grade, VGF growth, single crystal, orientation (100) ± 0.1°, undoped, single side polished, 3" diameter, 625 ± 25 μm thickness. Unless otherwise specified, chemicals were purchased from Sigma–Aldrich. PBS (phosphate-buffered saline 1x, pH 7.4), BupH™ MES (2-(N-Morpholino) ethanesulfonic acid) buffered saline pack, and NeutrAvidin™ biotin-binding protein (neutravidin) were purchased from Fisher Scientific. Sulfo-NHS (N-hydroxysulfosuccinimide sodium salt) and the photocrosslinker reagent, 3-[4-(Aminomethyl) phenyl]-3-(trifluoromethyl)-3H-diazirine hydrochloride (CAS 1258874–29-1), were purchased from Tokyo Chemical Industry. Endosulfin alpha (ENSA) (human, recombinant) protein with a polyhistidine tag at the N-terminus (His_6-ENSA protein) was purchased from SinoBiological. Solvents of ACS grade were used.

2.2. Methods

2.2.1. Samples preparation

GaAs wafers were cleaved into 0.5 cm x 0.5 cm pieces using a diamond scriber. Samples were cleaned with subsequent ultrasonic baths (5 min each) in acetone, ethanol and isopropanol, respectively, and dried with N_2 flow. Immediately before samples functionalisation with thiols, the GaAs oxide layer was removed by an acidic bath (2 min in HCl 1.0 N) followed by rinsing with water and ethanol. For **SAM formation**, the samples were incubated in a freshly prepared thiol solution for 24 h, under gentle agitation (by means of an orbital shaker). A mixture of ethanol and water (2:1) with 10 % (v/v) of acetic acid was used as solvent for the two thiols: carboxyl-OEG-thiol (CAS 866889–02-3) and hydroxyl-OEG-thiol (CAS 130727–41-2). The thiols were in solution at a final concentration of 95 μM for the carboxyl-OEG-thiol and 5 μM for the hydroxyl-OEG-thiol. The carboxyl groups are used for the immobilisation of the photocrosslinker molecule via carbodiimide crosslinking, with the hydroxyl groups act as spacers. After SAM formation, the samples were rinsed with the same solvent mixture and dried with N_2 flow.

For the **attachment of the photocrosslinker** molecule, the samples were incubated for 30 min in a freshly prepared mixture of N-hydroxysulfosuccinimide (sulfo-NHS) and N-(3-Dimethylaminopropyl)-N'-ethylcarbodiimide hydrochloride (EDC) in MES 0.1 M, pH 4.7. The final concentration of sulfo-NHS in solution was 50 mM, and EDC final concentration was 200 mM. The samples were thoroughly rinsed with the same buffer (MES) to remove excess products and by-products. Afterwards, the samples were rinsed with PBS to raise the surface pH and then incubated with the photocrosslinker solution (50 μg/L in PBS) for 2 h. The samples were then rinsed with flowing PBS and dried with N_2 flow.

To demonstrate the feasibility of this photochemical approach for multiplexed functionalisation, we promoted the **immobilisation of two proteins on the same GaAs sample** in two different regions of the sample, as illustrated in Fig. 1. The sample functionalised with photocrosslinker was firstly covered with a drop of neutravidin solution (50 μg/mL of protein diluted in PBST, i.e. PBS with 0.05 % TWEEN®20, pH 6.3) and then area A was exposed

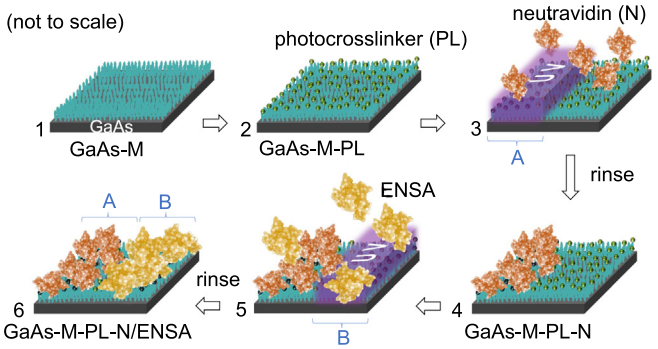

Fig. 1. Functionalisation strategy for the immobilisation of two proteins, neutravidin and Ni-ENSA, on selected areas (A and B) of a GaAs sample upon localised UV exposure. This strategy involves the creation of a monolayer (M) (1), followed by the immobilisation of a photoreactive crosslinker (PL) (2); the sample is then covered with neutravidin solution and area A is selectively exposed to long wavelength UV light (3) for activation of the PL; after rinsing, the unbound neutravidin molecules are removed from the surface, leaving area A functionalised with neutravidin (4); the sample is then covered with ENSA solution and area B is selectively exposed to UV (5) for PL activation and reaction with the protein; after rinsing, the unbound molecules of ENSA are removed from the surface, leaving area B functionalised with ENSA.

to UV, while area B remained protected from UV exposure by being covered with aluminium foil. In this way, only the photocrosslinker molecules in region A have been activated, resulting in the immobilisation of neutravidin in this area. After thorough rinse with a sequence of PBST and PBS (2 mL PBST flow followed by 4 x 2 mL PBS flow, then repeating 3 times), and drying with N2 flow, the sample was then covered with the Ni-ENSA protein solution and area B was exposed to UV, this time with area A being protected from UV (again by being covered with foil). Covering area A was required to avoid attachment of Ni-ENSA to available PL groups in this area, as they maintain their binding capability if they did not react in a previous exposure (see SI Sec. 4). The sample was then rinsed (PBST and PBS washes as described above) and dried with N_2 flow.

The Ni-ENSA protein solution was prepared by mixing equal volumes of His_6-ENSA protein (100 ug/mL in PBS) and $Ni(NO_3)_2$ (0.8 mM aqueous solution), and leaving it overnight under gentle agitation by means of an orbital shaker. Even if unreacted residual $Ni(NO_3)_2$ is present in the protein solution, it is unlikely that such molecules attach to the activated carbene, as the preferable reactions for this group are insertions into CH bonds. The samples were exposed to UV for 8 min (LED 365 nm; intensity measured at sample position: 0.24 W/cm^2, equivalent to an exposure dose of 115 J/cm^2 for 8 min exposure time) while fully covered with a drop of protein solution (either neutravidin or Ni-ENSA). The concentration of the protein in solution and the exposure time were optimised to obtain the highest protein coverage and limit the non-specific adsorption of protein on the surface (see SI, Table S1).

Table 1 summarises the samples analysed at different stages of functionalisation.

2.2.2. X-ray Photoelectron Spectroscopy (XPS)

XPS measurements were performed using a Thermo Scientific K-alpha$^+$ system with a monochromatic Al Kα source (1486.68 eV). Charge compensation (at low power, to avoid degradation) was applied to prevent sample charging. An X-ray spot size of 400 μm and take-off angle of 90 degrees were used. High resolution spectra were acquired at a pass energy of 40 eV (20 scans, dwell time 0.05 s). CasaXPS software (version 2.3.23rev1.1 N) was used for peak fitting using a least-squares method. For each selected region of a scan, either linear or 2 parameter Tougaard (so called U2 Tougaard) backgrounds were applied and peak models were created using LA (Lorentzian asymmetric) lineshapes [26,27], which provided a good fit to the data, i.e. low residual standard deviation values (see SI, Table S3).The corrected peak areas were calculated by the software and include Scofield cross-sections, a transmission function correction and an escape depth correction. The Scofield cross-sections are used to scale photoelectron peak areas to account for differences in peak intensity due to the scattering of electrons by photons of a given energy. Since photo-emitted electrons are subject to inelastic scattering before escaping the surface while travelling to the detection system, an escape depth correction is also necessary and this was achieved by dividing the peak intensity by KE$^{0.6}$, with KE being the kinetic energy. This value assigned for the escape depth correction is commonly used for Thermo Scientific XPS instruments. For the calculation of the C 1s spectral components, the position (i.e. binding energy) of each component was fixed and the full width at half maximum (FWHM) was constrained to be the same for all the components [28]. The area for the N 1s component was calculated by applying position and FWHM constrains (allowing to move ± 0.2 eV) to the overlapping peaks coming from the substrate. These were assessed from the GaAs-M (#1) scans and also verified by a high resolution scan of GaAs acquired just after in situ oxide layer removal with argon clusters [25].

Table 1
Overview of the samples investigated. M denotes monolayer, PL photocrosslinker, N neutravidin. ENSA refers to Ni-ENSA. #3 was divided in two areas (A and B), each of them being exposed to UV while incubated with a distinct protein (neutravidin or Ni-ENSA), as illustrated in Fig. 1.

ID	Stage
#1	GaAs-M
#2	GaAs-M-PL
#3A	GaAs-M-PL-**N(UV)**-ENSA(no UV)
#3B	GaAs-M-PL-N(no UV)-**ENSA(UV)**
#4	GaAs-M-PL-ENSA(no UV)
#5	GaAs-M-PL-N(no UV)

3. Results

XPS analysis was used as evidence of GaAs functionalisation by providing chemical information of the outmost surface layer at each functionalisation step. To differentiate between the two biomolecules - neutravidin and ENSA protein - we promoted the binding of nickel ions [29,30] to the hexahistidine (His_6)-tagged ENSA protein. In this way, nickel acted as a XPS marker for the ENSA protein, while being absent for neutravidin. A schematic representation of the functionalisation strategy followed in this study is shown in Fig. 2. The spatially localised attachment of the analyte receptor is achieved by preventing the illumination of the crosslinker by using an opaque mask.

3.1. SAM formation and immobilisation of the photocrosslinker

The GaAs surface was firstly functionalised with dual-component oligo(ethyl glycol)-containing (OEG)- alkanethiolate films, the first component being a hydroxyl-OEG-thiol and the second a carboxyl-OEG-thiol (molecular structures shown in Fig. S2). The carboxyl groups displayed on the surface were then used for covalent attachment of the photocrosslinker (PL) molecule via carbodiimide crosslinking chemistry, while the hydroxyl chains function was to act as spacer molecules (molecular structures shown in Fig. S3). The characterisation of a dual-component SAM formed from these 2 thiols, using an equimolar thiol solution, has been previously reported by us [25]. In the study here reported, a solution with higher molar fraction of the carboxyl-OEG-thiol (0.95) was used. This choice was based on wettability experiments that showed lower amount of protein attached to the surface (after activation of the photocrosslinker) for the SAM formed from an equimolar thiol solution, when compared to the carboxyl-enriched SAM (see SI, Fig. S4).

High resolution XPS scans acquired for the SAM formed on GaAs (#1) and further immobilisation of the photocrosslinker (#2) are shown in Fig. 3. Table 2 shows the ratios of the areas of the N 1s

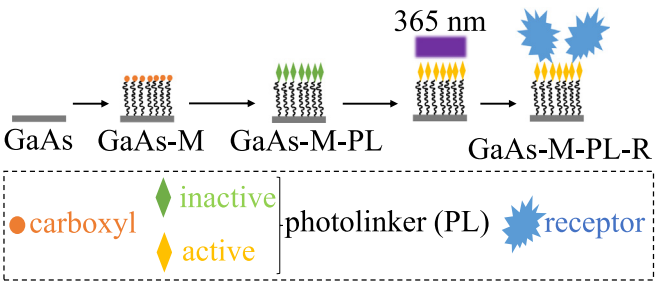

Fig. 2. Light-facilitated immobilisation of biomolecules on GaAs. This strategy involves the immobilisation of a photoreactive crosslinker (PL) onto a monolayer (M) exhibiting carboxyl groups, followed by localised exposure to long wavelength UV light for attachment of the desired bio-receptor (R).

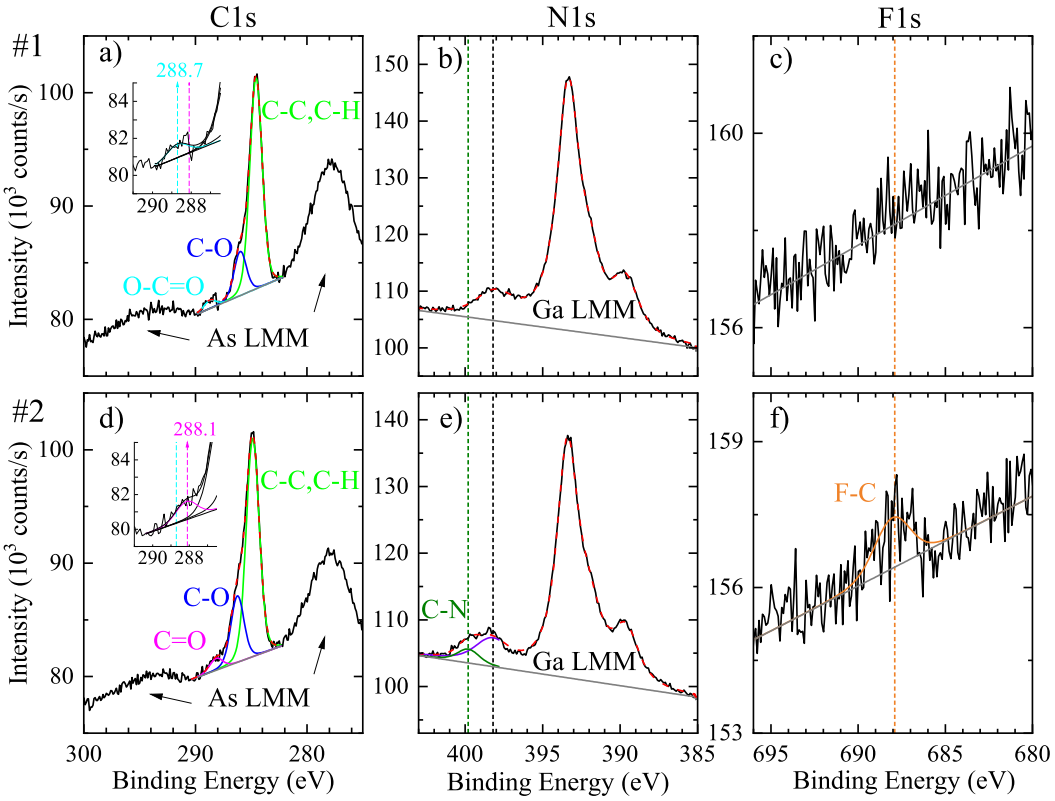

Fig. 3. XPS high resolution scans for C 1s (a, d), N 1s (b, e) and F 1s (c, f) spectral regions for stage #1 (top row: a-c) and #2 (bottom row: d-f), respectively. The background baseline is shown in grey. Fitted components for C 1s include C – C and C – H (green), C – OH, C – O–C and C – N (blue), C = O (magenta) and O – C = O (cyan), respectively, with the dashed red line being their sum; this region is overlapped by As LMM Auger peaks (not fitted). The inset plot in a) is a magnification of the O – C = O peak fitting and the inset plot in d) is a magnification of the C = O peak fitting, the vertical dashed lines showing the binding energies of each peak. The N 1s region includes the fit for C-N (green), overlapped by Ga LMM Auger peaks (also fitted), with the dashed red line being their sum. Additional plots for the N 1s region are shown in SI, Fig. S5.

Table 2
Ratio of N 1s, C 1s and Ni $2p_{3/2}$ to Ga $2p_{3/2}$. These were calculated from the fitted peak areas (corrected for the transmission function, mean free path and sensitivity factors) of XPS high resolution scans. The values are the average of measurements on triplicate samples, with the errors representing the standard deviation. Where no evident peak was present, an upper limit for the ratio was estimated by fitting a peak to the residual; these values are shown in brackets.

Stage	$\frac{N\,1s}{Ga\,2p_{3/2}}$	$\frac{C\,1s}{Ga\,2p_{3/2}}$	$\frac{Ni\,2p_{3/2}}{Ga\,2p_{3/2}}$	$\frac{C\,1s}{N\,1s}$
#1	(-)	1.28 ±0.47	(-)	
#2	0.09 ±0.01	1.77 ±0.48	(-)	19.4
#3A	0.29 ±0.12	1.89 ±0.74	0.01 ±0.01	6.6
#3B	0.94 ±0.19	6.19 ±0.16	0.23 ±0.03	6.6
#4	0.42 ±0.09	3.52 ±0.23	(0.006)	8.4
#5	0.08 ±0.04	2.40 ±0.32	(-)	30.3

and C 1s to Ga $2p_{3/2}$ peaks, while the C 1s component ratios, calculated from the high resolution scans, are given in Table 3. Additional XPS data fit parameters can be found in SI (Table S2 and Table S3).

The presence of carboxyl groups on the surface after SAM formation is confirmed by the C 1s component at ~289 eV [31] (Fig. 3a). As expected, there is no nitrogen present on this surface, as this element is not a constituent of the thiol molecules (SI, Fig. S2), with the Ga LMM auger components [32] - which overlap the N 1s region - being the only peaks observed here (Fig. 3b). The absence of fluorine, element only present in the photocrosslinker molecule, was also confirmed (Fig. 3c). Scans acquired for the S 2p region constitute additional evidence of SAM formation (shown in SI, Fig. S6).

Table 3
C 1s relative component percentages, showing the bonds assigned to each component, with C1 detected at 284.8 eV, C2 detected at 286.2 eV, C3 detected at 288.1 eV and C4 detected at 289.0 eV. These relative ratios were calculated from the fitted peak areas (corrected for the transmission function, mean free path and sensitivity factors) of XPS high resolution scans. The values are the average of measurements on triplicate samples, with the errors representing the standard deviation. Where no evident peak was present, an upper limit for the ratio was estimated by fitting a peak to the residual; these values are shown in brackets.

Stage	C 1*s* components			
	C_1 C – C C – H	C_2 C – OH, C – N C – O – C	C_3 C = O	C_4 O – C = O
#1	77 ±5	20 ±3	0	3 ±1
#2	72 ±2	23 ±1	5 ±2	(0.6)
#3A	63 ±4	23 ±2	13 ±3	1 ±1
#3B	59 ±1	23 ±0	17 ±1	1 ±1
#4	55 ±2	30 ±0	15 ±1	(-)
#5	63 ±4	32 ±3	4 ±1	(-)

The successful immobilisation of the photoreactive crosslinker via carbodiimide crosslinking is demonstrated by the presence of nitrogen (Fig. 3e, with additional stacked plots shown in SI, Fig. S5) and the presence of a modest fluorine peak at 687.6 eV (Fig. 3f), assigned to an organic fluorine [33]. In addition, the C 1s component assigned to O – C = O bonds is not observed in #2, being replaced by the component assigned to C = O bonds, as a result of the crosslinking reaction of the carboxyl groups with the amine groups of the photocrosslinker molecule via carbodiimide chemistry. The components corresponding to the CF_3 group [34] and the π-π^* transition shake-up [35] from the photocrosslinker aromatic ring, expected at 292.5 eV and 291 eV, overlap with the As LMM Auger peak [36] (not fitted).

3.2. Multiplexed spatially selective immobilisation of proteins

Two distinct proteins, neutravidin and Ni-ENSA, were immobilised on the GaAs surface by spatially selective activation of the photocrosslinker upon exposure to UV light (Fig. 1).

XPS high resolution scans for #3A and #3B are shown in Fig. 4, focusing on C 1s, N 1s and Ni 2p regions, to demonstrate protein attachment. The correspondent ratios of the peak areas are shown in Table 2, while the C 1s component ratios are given in Table 3.

The attachment of the proteins is confirmed by an increase in C to Ga and N to Ga ratios and also by a dramatic change in the C to N ratio, comparing with the surface functionalised with PL (#2).

While a theoretical ratio of C to N close to 3 is expected for a neutravidin molecule, this ratio is of 9.6 for the surface where the PL is attached to the monolayer (see molecular structure shown in Fig. S3), assuming each carboxyl group reacted with a PL molecule and taking into account the 0.05 M fraction of hydroxyl-OEG-thiol in solution when creating the mixed monolayer. Therefore, a decrease factor of ~ 3.2 is expected after protein attachment, if neglecting signal contribution from the layers underneath. A reduction factor of 2.9 (as a result of the ratio of the XPS relative areas for the C 1s and N 1s peak for the sample #2 (19.4) and #3 (6.6)) was observed, in line with the expected. The relative ratio of carbon components also changed after protein attachment, with an increase of C = O bonds being observed. The negligible amount of Ni (Fig. 4c) suggests the absence of Ni-ENSA on #3A, while the presence of a prominent peak Ni on #3B (Fig. 4f) confirms the attachment of the Ni-ENSA on area B after UV exposure. These results suggest the efficiency of the photocrosslinker activation under UV exposure and its reaction with the proteins and demonstrate the success of this functionalisation strategy for the spatially selective attachment of two distinct proteins on the GaAs surface.

The higher ratio of C to Ga and N to Ga observed for #3B comparing with #3A (Table 2) indicates that the surface coverage with protein is higher for area B. Ni-ENSA is a smaller protein than neutravidin (18 kDa vs. 60 kDa) which might contribute for a higher amount of this protein being attached to the surface as a result of less steric hindrance effects. In addition, there might be a contribution from non-specific binding, discussed below.

3.3. Non-specific binding

The presence of non-specific binding of the proteins onto the layer functionalised with PL was investigated by incubating this surface with the protein solution (Ni-ENSA solution for #4 and

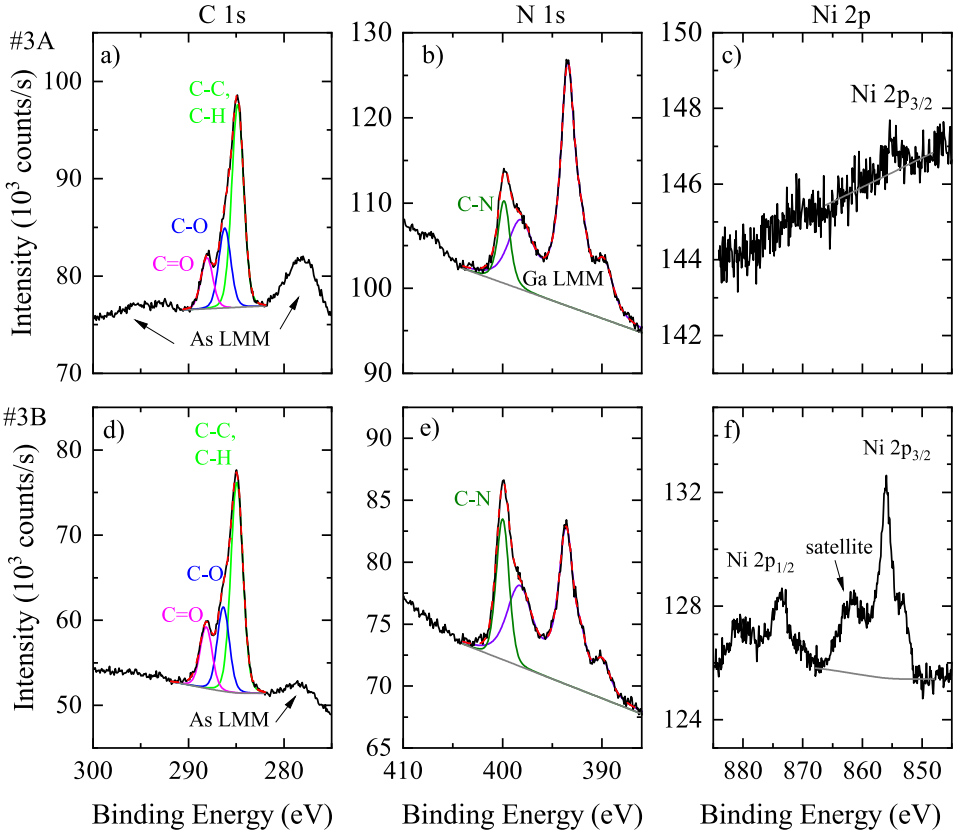

Fig. 4. XPS high resolution scans for C 1s (a, d), N 1s (b, e) and Ni 2p (c, f) regions for two distinct areas of sample #3, A (top row: a-c) and B (bottom row: d-f), where A was exposed to UV light while covered with neutravidin solution, and B was exposed to UV light while covered with Ni-ENSA solution. The background baseline is shown in grey. Fitted components for C 1s include C – C and C – H (green), C – OH, C – O–C and C – N (blue), C = O (magenta) and O – C = O (cyan), respectively, with the dashed red line being their sum; this region is overlapped by As LMM Auger peaks (not fitted). The N 1s region includes the fit for C-N (green), overlapped by Ga LMM Auger peaks (also fitted), with the dashed red line being their sum. The Ni $2p_{3/2}$ peak region, overlapped by a satellite [37], was used for quantification of this element.

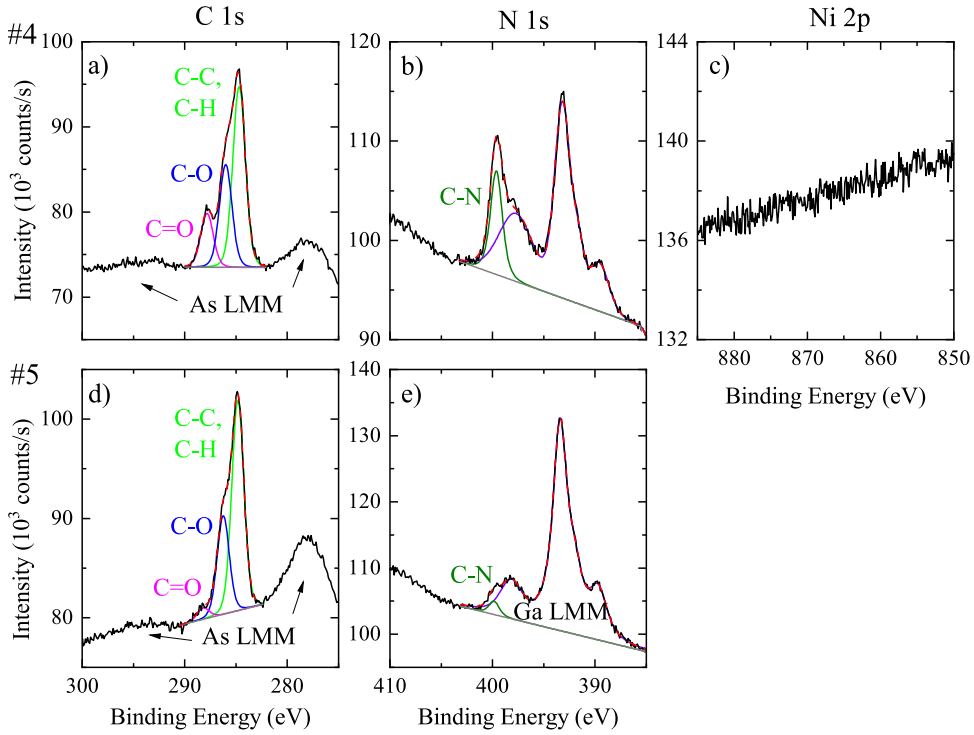

Fig. 5. XPS high resolution scans for C 1s (a, d), N 1s (b, e) and Ni 2p (c) regions for stage #4 (top row: a-c) and #5 (bottom row: d, e), respectively. The background baseline is shown in grey. Fitted components for C 1s include C − C and C − H (green), C − OH, C − O−C and C − N (blue) and C = O (magenta), respectively, with the dashed red line being their sum; this region is overlapped by As LMM auger peaks (not fitted). The N 1s region includes the fit for C-N (green), overlapped by Ga LMM auger peaks (also fitted), with the dashed red line being their sum.

neutravidin solution for #5) without UV light exposure, i.e. without activating the photocrosslinker. XPS high resolution scans for these are shown in Fig. 5 and elemental ratios in Table 2 and Table 3.

Despite the absence of Ni, the increase in N to Ga and C to Ga ratios observed for control #4 comparing with #2, suggests that a certain amount of Ni-ENSA is attached to the surface. However, this is a lower amount of protein attachment comparing with #3B, exposed to UV light, since the observed ratios of N to Ga and C to Ga are smaller in the absence of UV light exposure. The fact that no Ni is visible might be an indication that the protein adopts a different conformation when attached non-specifically (by means of electrostatic interactions, for example) comparing with the attachment via the photocrosslinker. The absence of Ni in XPS scans concerning low surface concentration of Ni-tagged proteins has been previously reported [38].

Conversely, the results for control #5 suggest the absence of non-specific binding of neutravidin onto the layer functionalised with PL, as the N to Ga ratio is similar to the one observed for #2. It is important to note that the pH of the rinsing buffer was selected in accordance with the isoelectric point (pI) of neutravidin (6.3). This is likely to be the reason why this buffer is more effective in reducing non-specific binding of neutravidin, and highlights the importance of optimising the washing procedure in accordance with the bioreceptor being immobilised.

4. Conclusions

This is the first study reporting the spatially localised functionalisation of GaAs with multiple biomolecules. Based on XPS analysis, we have demonstrated the feasibility of using a diazirine derivative photocrosslinker for immobilising two different proteins on different selected areas of GaAs surface, using UV light as the facilitator. The method can be easily expanded to multiple bioreceptors with an expected spatial resolution of $\lesssim$350 nm using a standard lithography approach. The use of Ni as a marker for the ENSA protein allowed the confirmation of site specificity for this method. The functionalisation method here described can be followed for the covalent attachment of a wide range of biomolecules and the dual-component SAM offers flexibility for controlling the density of biomolecules on the surface. We expect that given GaAs optoelectric properties, this study can be a valuable tool for the development of GaAs biosensors with multiplexed capability.

5. CRediT authorship contribution statement

Bárbara Santos Gomes: Writing (original draft), Conceptualisation, Methodology, Investigation; **Francesco Masia**: Supervising, Conceptualisation, Validation, Writing (reviewing and editing).

Declaration of Competing Interest

The authors declare that they have no known competing financial interests or personal relationships that could have appeared to influence the work reported in this paper.

Acknowledgements

This research was supported by the Ser Cymru II programme (Case ID 80762-CU-148) which is part-funded by Cardiff University and the European Regional Development Fund through the Welsh Government. XPS data collection was performed at the EPSRC National Facility for XPS (HarwellXPS), operated by Cardiff University and UCL, under contract No. PR16195. We thank David Morgan (School of Chemistry, Cardiff Catalysis Institute, UK) for running the XPS measurements and Maria White for preparing samples with protein immobilised on varying carboxyl-thiol molar fractions, shown in SI. We also thank Neal Fairley from CasaXPS for the support provided regarding the use of CasaXPS software for

data analysis. Discussions with Wolfgang Langbein and Paola Borri are gratefully acknowledged.

Appendix A. Supplementary material

Supplementary data associated with this article can be found, in the online version, at https://doi.org/10.1016/j.jcis.2022.06.071.

References

[1] G. Dorman, G. Prestwich, Using photolabile ligands in drug discovery and development, Trends Biotechnol. 18 (2000) 299–312.
[2] M. Neves-Petersen, G. Gajula, S. Petersen, Molecular Photochemistry - Various Aspects; InTech, 2012, pp. 125–158.
[3] C.L. Hypolite, T.L. McLernon, D.N. Adams, K.E. Chapman, C.B. Herbert, C.C. Huang, M.D. Distefano, W.S. Hu, Formation of microscale gradients of protein using heterobifunctional photolinkers, Bioconjug. Chem. 8 (1997) 658–663.
[4] S. Berneschi, F. Baldini, A. Cosci, D. Farnesi, G. Nunzi Conti, S. Tombelli, C. Trono, S. Pelli, A. Giannetti, Fluorescence biosensing in selectively photo–activated microbubble resonators, Sens. Actuat., B: Chem. 242 (2017) 1057–1064.
[5] H. Gao, R. Luginbühl, H. Sigrist, Bioengineering of silicon nitride, Sens. Actuat., B: Chem. 38 (1997) 38–41.
[6] A.L. MacKinnon, J.L. Garrison, R.S. Hegde, J. Taunton, Photo-leucine incorporation reveals the target of a cyclodepsipeptide inhibitor of cotranslational translocation, J. Am. Chem. Soc. 129 (2007) 14560–14561.
[7] J. Das, Aliphatic diazirines as photoaffinity probes for proteins: Recent developments, Chem. Rev. 111 (2011) 4405–4417.
[8] G. Hermanson, The Reactions of Bioconjugation. Bioconjugate Techniques, 2013
[9] V. Lacour, E. Herth, F. Lardet-Vieudrin, J. Dubowski, T. Leblois, GaAs based on bulk acoustic wave sensor for biological molecules detection, Proc. Eng. 120 (2015) 721–726.
[10] M. Aziziyan, W. Hassen, D. Morris, E. Frost, J. Dubowski, Photonic biosensor based on photocorrosion of GaAs/AlGaAs quantum heterostructures for detection of Legionella pneumophila, Biointerphases 11 (2016) 019301.
[11] Y. Cho, A. Ivanisevic, Covalent Attachment of TAT Peptides and Thiolated Alkyl Molecules on GaAs Surfaces, J. Phys. Chem. B 109 (2005) 12731–12737.
[12] E. Nazemi, W. Hassen, E. Frost, J. Dubowski, Growth of Escherichia coli on the GaAs (001) surface, Talanta 178 (2018) 69–77.
[13] V. Duplan, Y. Miron, E. Frost, M. Grandbois, J. Dubowski, Specific immobilization of influenza A virus on GaAs (001) surface, J. Biomed. Opt. 14 (2009) 054042.
[14] A. Bienaime, T. Leblois, N. Gremaud, M.-J. Chaudon, M. Osta, D. Pecqueur, P. Ducoroy, C. Elie-Caille, Influence of a Thiolate Chemical Layer on GaAs (100) Biofunctionalization: An Original Approach Coupling Atomic Force Microscopy and Mass Spectrometry Methods, Materials 6 (2013) 4946–4966.
[15] C. Sheen, J. Shi, J. Martensson, A. Parikh, D. Allara, A New Class of Organized Self-Assembled Monolayers: Alkane Thiols on GaAs (100), J. Am. Chem. Soc. 114 (1992) 1515–1517.
[16] C. McGuiness, A. Shaporenko, C. Mars, S. Uppili, M. Zharnikov, D. Allara, Molecular Self-Assembly at Bare Semiconductor Surfaces: Preparation and Characterization of Highly Organized Octadecanethiolate Monolayers on GaAs (001), J. Am. Chem. Soc. 128 (2006) 5231–5243.
[17] C. McGuiness, A. Shaporenko, M. Zharnikov, A. Walker, D. Allara, Molecular Self-Assembly at Bare Semiconductor Surfaces: Investigation of the Chemical and Electronic Properties of the Alkanethiolate-GaAs(001) Interface, J. Phys. Chem. C 111 (2007) 4226–4234.
[18] P. Mancheno-Posso, A. Muscat, Self-assembly of alkanethiolates directs sulfur bonding with GaAs(100), Appl. Surf. Sci. 397 (2017) 1–12.
[19] V. Lacour, K. Moumanis, W. Hassen, C. Elie-Caille, T. Leblois, J. Dubowski, Formation Kinetics of Mixed Self-Assembled Monolayers of Alkanethiols on GaAs(100), Langmuir 35 (2017) 4415–4427.
[20] Y. Jun, X. Zhu, J. Hsu, Formation of Alkanethiol and Alkanedithiol Monolayers on GaAs(001), Langmuir 22 (2006) 3627–3632.
[21] O. Voznyy, J. Dubowski, Structure of thiol self-assembled monolayers commensurate with the GaAs (001) surface, Langmuir 24 (2008) 13299–13305.
[22] R. St-Onge, J. Vermette, W.M. Hassen, Formation of extraordinary density alkanethiol self-assembled monolayers on surfaces of digitally photocorroded (001) GaAs/AlGaAs nanoheterostructures, Appl. Phys. Lett. 118 (2021).
[23] H. Moteshareie, W.M. Hassen, J. Vermette, J.J. Dubowski, A.F. Tayabali, Strategies for capturing Bacillus thuringiensis spores on surfaces of (001) GaAs-based biosensors, Talanta 236 (2022) 122813.
[24] O. Voznyy, J. Dubowski, Adsorption Kinetics of Hydrogen Sulfide and Thiols on GaAs (001) Surfaces in a Vacuum, J. Phys. Chem. C 112 (2008) 3726–3733.
[25] B. Santos Gomes, D.J. Morgan, W. Langbein, P. Borri, F. Masia, Biofunctionalisation of gallium arsenide with neutravidin, J. Colloid Interface Sci. 608 (2021) 2399–2406.
[26] G. Major, D. Shah, V. Fernandez, N. Fairley, M. Linford, Advanced Line Shapes in X-Ray Photoelectron Spectroscopy I. The Asymmetric Lorentzian (LA) Line Shape, Vacuum Technol. Coat. (2020) 43–46.
[27] N. Fairley, CasaXPS Manual 2.3.15 Rev1.2, 2009.
[28] T.R. Gengenbach, G.H. Major, M.R. Linford, C. Easton, Practical guides for x-ray photoelectron spectroscopy (XPS): Interpreting the carbon 1s spectrum Practical guides for x-ray photoelectron spectroscopy (XPS): Interpreting the carbon 1s spectrum, J. Vacuum Sci. Technol. A (2021) 013204.
[29] L.M. Franklin, S.M. Walker, G. Hill, A DFT study of isolated histidine interactions with metal ions (Ni2+, Cu2+, Zn2+) in a six-coordinated octahedral complex, J. Mol. Model. (2020) 26.
[30] L.E. Valenti, C.P. De Pauli, C.E. Giacomelli, The binding of Ni(II) ions to hexahistidine as a model system of the interaction between nickel and His-tagged proteins, J. Inorg. Biochem. 100 (2006) 192–200.
[31] C. Wagner, W. Riggs, L. Davis, J. Moulder, In Handbook of X-ray Photoelectron Spectroscopy; Muilenberg, G., Ed.; Perkin-Elmer Corp. Physical Electronics Division, 1979.
[32] E. Antonides, E. Janse, G. Sawatzky, LMM Auger spectra of Cu, Zn, Ga and Ge. Transition probabilities, term splittings and effective Coulomb interaction, Phys. Rev. B 15 (1977) 1669–1679.
[33] M.P. Hernández, G. Navarro-Marín, O. Estévez-Hernández, M.H. Farías Sánchez, Angle-resolved X-ray photoelectron spectroscopy study of the thiourea derivative adsorption on Au(111) from ethanolic solution, Revista Cubana de Fisica 34 (2017) 108–111.
[34] D. Léonard, Y. Chevolot, O. Bucher, H. Sigrist, H. Mathieu, ToF-SIMS and XPS study of photoactivatable reagents designed for surface glycoengineering: Part I. N-(m-(3-(trifluoromethyl)diazirine-3-yl)phenyl)-4-maleimido-butyramide (MAD) on silicon, silicon nitride and diamond, Surf. Interface Anal. 26 (1998) 783–792.
[35] M.C. Evora, J.R. Araujo, E.H. Ferreira, B.R. Strohmeier, L.G. Silva, C.A. Achete, Localized surface grafting reactions on carbon nanofibers induced by gamma and e-beam irradiation, Appl. Surf. Sci. 335 (2015) 78–84.
[36] E. Roberts, P. Weightman, C. Johnson, Photoelectron and L2,3 MM Auger electron energies for arsenic, J. Phys. C: Solid State Phys. 8 (1975) 1301–1309.
[37] A.P. Grosvenor, M.C. Biesinger, R.S.C. Smart, N.S. McIntyre, New interpretations of XPS spectra of nickel metal and oxides, Surf. Sci. 600 (2006) 1771–1779.
[38] E. Kang, J.W. Park, S.J. McClellan, J.M. Kim, D.P. Holland, G.U. Lee, E.I. Franses, K. Park, D.H. Thompson, Specific adsorption of histidine-tagged proteins on silica surfaces modified with Ni2+/NTA-derivatized poly(ethylene glycol), Langmuir 23 (2007) 6281–6288.